Lešnik, L., Palomar-Torres, A., Torres-Jiménez, E., Mata, C., Valh, J. V., Kevorkijan, L., & Biluš, I. (2022). The effect of HDPE and LDPE pyrolytic oils on cavitation formation in a common-rail diesel injector. Fuel, 330, 125581. https://doi.org/10.1016/j.fuel.2022.125581

The effect of HDPE and LDPE pyrolytic oils on cavitation formation in a common-rail diesel injector

L. Lešnik[1*], A. Palomar-Torres[2], E. Torres-Jiménez[2], C. Mata[3], J. Volmajer Valh[1], L. Kevorkijan[1] and I. Biluš[1]

[1.] University of Maribor, Faculty of Mechanical engineering, Smetanova ulica 17, SI-2000 Maribor, Slovenia.

[2.] Dept. of Mechanical and Mining Engineering, University of Jaén, Campus las Lagunillas, s/n, 23071 Jaén, Spain.

[3.] Universidad de Castilla-La Mancha, Campus de Excelencia Internacional en Energía y Medioambiente, Escuela de Ingeniería Minera e Industrial de Almadén, Plaza Meca s/n, 13400 Almadén, Spain

*Corresponding authors at: University of Maribor, Faculty of Mechanical Engineering, Maribor, Slovenia. E-mail addresses: luka.lesnik@um.si (Luka Lešnik)

Abstract

Plastic production and usage increase every year due to its practicality, adaptability, and low-cost production. The problem with plastic arises when it becomes waste and needs to be treated. Most of the plastic we use is produced from petrochemical material that can be used in resource recovery processes like pyrolysis to produce various materials. One of the pyrolysis process products is pyrolytic oil, whose properties are similar to conventional fuels. Minor differences in fuel properties can influence the injection process, in-nozzle flow condition, spray formation and break-up, the combustion process, etc. The presented paper aims to study the influence of pyrolytic oil`s properties on cavitation formation in the injection nozzle of a common-rail injector. First, the pyrolytic oils were

obtained from waste high- and low-density polyethylene using a pyrolysis reactor. Afterwards, the oils were characterized and implemented in the AVL FIRE computation program for studying their influence on cavitation formation in the injection nozzle hole. The obtained results indicate slight differences in fuel properties that influence cavitation formation and spread in the injection hole, which further influence conditions at the exit of the injection hole. The lower lower viscosity of pyrolytic oils influences lower friction in the fuel nozzle flow. The lower densyt and viscosity of pyrolytic oils promotes cavitation formation, advance time of it appearance at injection hole exit and influence the shorter presence of cavitation in the needle closing phase.

Key words: plastic waste, pyrolytic oils, cavitation, common-rail, multiphase flow, transient simulation

Introduction

Plastic and plastic products play a significant role in our everyday life. Several traditional materials like steel, wood, etc., have been replaced by plastic materials. This has influenced the rapid increase of plastic production in the recent decade, which reached 368 million tonnes globally in 2019, from which Europe encountered the production of 57.9 million tons of produced plastic. [1] Low production costs, rapid economic growth, and the increase in global populations, are only a few reasons for the constant global growth in plastic production. [2]. Globally, the plastic production compound annual growth rate is 8.4 %. [3] [4]. More than half of global plastic is produced in Asian countries, while Europe was responsible for 16 % of the total global plastic production in 2019. The problem with plastic arises when it becomes waste that needs to be treated. There are several techniques that can be employed for plastic waste treatment. The most conventional process for plastic waste treatment is landfilling, which is still used commonly nowadays. According to [5], about 40 % of plastic waste ends in landfill globally. The problem with landfilling of plastic waste is the non-biodegradability nature of plastic materials, which will degrade very slowly in landfill conditions. Additionally, small particles of degraded plastic can come in contact with groundwaters which can

lead to contamination of water sources, air, or soil. [6] In Europe, 24.9 % of collected plastic waste was sent to landfilling in 2018, 42.6 % of collected waste plastic was used in energy recovery processes, and 32.5 % was sent to recycling. [1] Waste plastic recycling can be divided further into physical recycling and resource recovery, attracting increasing attention, since it can help us to obtain expensive petrochemical materials that can also be used as fuels. The process of resource recovery is realized mainly using thermolysis processes, from which pyrolysis is used most widely. [7] Pyrolysis is a process in which long-chain polymers are degraded into smaller, less complex molecules at elevated temperatures and in the absence of oxygen. The catalyst can be used further to influence the obtained oil properties. [8] [9] [10] The main products of plastic waste pyrolysis are oil, gas, and solid residue. [11] [12] Since most plastic is still produced from petrochemical materials, [7] the oil produced from plastic waste has properties similar to diesel and gasoline fuels, and can be used in internal combustion engines.

Kizza et al. used waste low-density polyethylene (LDPE), high-density polyethylene (HDPE), polypropylene (PP), and polystyrene (PS) to produce plastic derived fuels (PDF) using a pyrolysis process. The viscosity, density and flash point of the fuels were lower than diesel, while the lower heating value of PDF was in a similar range to diesel fuel. They concluded that the produced fuels compared relatively well with conventional diesel fuel properties in Uganda, and could potentially substitute it. [13] Tulashie et al. also used waste PP, HDPE and LDPE plastic to produce PDF using a batch fixed bed pyrolysis reactor. After the characterization, they observed that the obtained fuels properties were in the diesel fuel range, and concluded that pyrolysis of plastic waste presents an efficient and clean method for treating plastic waste. [14] The semi-batch pyrolytic reactor with fixed bed was also used in the study of Mangesh et al. [15] The waste plastic they used was the same as in the work of Tulashie et al. [14], while ZSP-5 zeolite was used as the catalyst. The results of catalytic pyrolysis indicate that some plastic derived fuels (oils) have properties that are very similar to conventional diesel fuel, while others differ slightly from diesel properties. Since the properties of PDF produced from PP plastics have the most diesel like characteristics, they used this oil to produce

a 5, 10, and 15% mixture of PP derived PDF with conventional diesel, and tested it in a 4-cylinder, turbocharged diesel engine. The obtained results indicate that the use of PDF from PP plastic as a substitute for conventional diesel leads to higher in-cylinder peak pressure, a higher heat release rate, higher brake specific fuel consumption, a higher exhaust gas temperature, a longer ignition delay and higher emissions of carbon monoxide (CO), carbon dioxide (CO2), nitrogen oxides (NOx), and hydrocarbons (HC). [15] Singh et al. [16] used LDPE plastic to produce pyrolytic oil in a fixed bed reactor, and used it to make a 20 % mixture of PDF with conventional diesel fuel. The mixture was used further to run a single-cylinder, naturally aspirated diesel engine, and the obtained results were compared to diesel and pure PDF fuel. The obtained results indicate that the use of pyrolytic oil has a minor influence on in-cylinder pressure, but it decreases engine brake thermal efficiency, increases exhaust gas temperature, CO emissions, HC emissions, NO_x emissions, while decreasing CO_2 emissions. Das et al. [17] used medical plastic waste to produce PDF in a batch pyrolysis reactor and used this oil further to run a compression ignition engine with different mixtures of PDF with diesel fuel. They concluded that pyrolytic oils influence engine brake thermal efficiency slightly, but increase CO emissions, HC emissions, NO_x emission, and CO_2 emissions. A similar effect on engine condition was also observed in [18], where mixed plastic was used to obtain pyrolytic oil in a reactor with a fixed bed.

As can be seen from the presented literature review, plastic waste can be transformed into synthetic fuels successfully via a pyrolysis process. Their usage in internal combustion engines influences engine performance and the emission formation process. This is usually related to the different chemical composition and physical properties of pyrolytic oils compared to conventional fuels. It is well known that diesel engine performance and the emission formation process are also related to the spray development and spray formation process, which can be affected by the fuel flow conditions in diesel injectors. [19] [20] The fuel flow conditions inside the injector nozzle can be influenced by the injection pressure, which is increased significantly in modern common rail injectors in order to obtain more efficient combustion and to increase engine efficiency. [21] Yu et al. [22]

concluded that higher viscosity of the fuel leads to lower cavitation formation inside the fuel injector. The fuel with the highest viscosity had the longest spray penetration length and the narrowest spray jet. [22] Torrelli et al. [23] tested the influence of fuel properties on internal nozzle flow in a five-hole injector. They concluded that fuel properties influence the injector performance and cavitation formation inside the injector. Less viscous fluids have lower friction, resulting in higher fuel velocities, and influencing their mass flow rate at the same pressure. Jiang et al. [24] also found that fuels with lower viscosity are more likely to form cavitation in an injector nozzle.

Since the difference in fuel properties can influence fuel flow conditions in a diesel injector nozzle significantly, the presented paper focuses on studying the influence of plastic-derived fuels` (pyrolytic oils) properties on the fuel flow conditions and cavitation inception in a Denso common-rail injector. The study was done using the 3D computational program AVL FIRE, in which transient simulations, which consider full needle movement during the fuel injections, were carried out using the RANS approach. First, the pyrolytic oils were obtained from HDPE and LDPE plastics using a batch reactor with a fixed bed in a nitrogen atmosphere. The obtained oils were characterized further and their properties were compared to conventional diesel fuel and implemented in a computational program. The numerical model was validated compared to the experimental results, and the proper computational mesh was selected in the next Section. Then, numerical simulations were performed using different mixtures of diesel fuel and pyrolytic oils at a constant injection pressure of 845 bar and a constant in-cylinder pressure of 60 bar. The same needle lift profile was used for all fuels. The obtained results indicate that the differences in fuel properties influence cavitation formation inside the injection hole and the condition at the injection hole exit.

To the authors' knowledge, the influence of pyrolytic oils on cavitation inception inside the injection nozzle has not been studied extensively. Therefore, we believe that the study can help to understand the behavior of pyrolytic oils on the condition inside the injection nozzle, and can bring their usage in compression ignition engines closer to their implementation.

Materials and methods

Plastic Material

The plastic used in the presented study was collected from municipal waste at the Faculty of Mechanical Engineering at the University of Maribor. The plastic waste was sorted, and only LDPE and HDPE plastics were used for obtaining oily pyrolytic. The collected plastic was washed and dried before it was cut into smaller pieces.

Pyrolysis Oil Production

A single batch pyrolytic reactor with a fixed bed was used for liquid oils` production in the presented study. The set of the pyrolysis process experiment is presented schematically in Figure 1. The used plastic waste was inserted into the reactor chamber, which was sealed and insulated with a glass wool jacket. The temperature inside the reactor was monitored using a K-type thermocouple and a National Instruments DAQ carrier WLS-9163 and NI-9219 module. Before each experiment, nitrogen gas (N2) was used to flush the whole system and to eliminate any potential air pockets out of system.

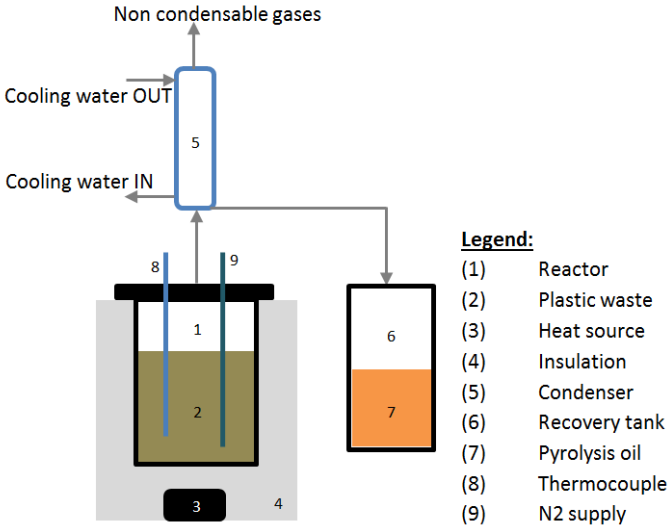

Figure 1: Pyrolysis process experiment set-up

The pyrolytic process was carried out at a 400°C reactor temperature. The produced vapors flow into the condenser, where the majority of it condenses. The obtained pyrolytic oils were collected in a

recovery tank and were removed at the end of the process. Non condensable gases were released into the atmosphere, and the solid residue was removed from the reactor chamber after each experiment.

Oils characterization

The properties of fuels play a significant role in their use. If fuels want to be used as road propulsion fuel for compression ignition engines in the European Union, they must meet the EN 590 Standard for diesel fuel. The following section of the manuscript presents some properties of the obtained PDF and their comparison to conventional diesel fuel.

The presented study does not focus on optimizing the pyrolysis process or decrease of energy consumption during the process, so the ratios of pyrolysis products and energy balance were not included in the presented work. The properties of the obtained pyrolytic oils from HDPE and LDPE plastics and the properties of diesel fuels required by the EN 590 Standard are presented in Table 1.

Table 1: Fuel properties [8]

	D2 EN 590	HDPE	LDPE
Density at 15°C [kg/m^3]	820-845	770.40	775.40
Surface tension [mN/m]	26.80	23.20	23.00
Calorific value [MJ/kg]	42.8-43.4	46.43	46.54
Kin. Viscosity [mm^2/s]	2.0-4.5	1.32	1.53
Cetan index	51.8	63.97	64.38
CHNO content [%w/w]	86.13 C	78.44 C	80.91 C
	13.87 H	13.40 H	13.53 H
	0 N	0.21 N	0.20 N
	0 O_2	7.94 O_2	5.35 O_2

Figure 2 presents the results of the carbon number distribution for the obtained pyrolytic oils. As can be seen from the results, the obtained oils consist of hydrocarbons with carbon numbers in the range C4 to C36, with the majority in the range of C6 to C19. This is in good agreement with diesel fuel, which has a carbon number distribution in the range from C8 to C23. [27][28]

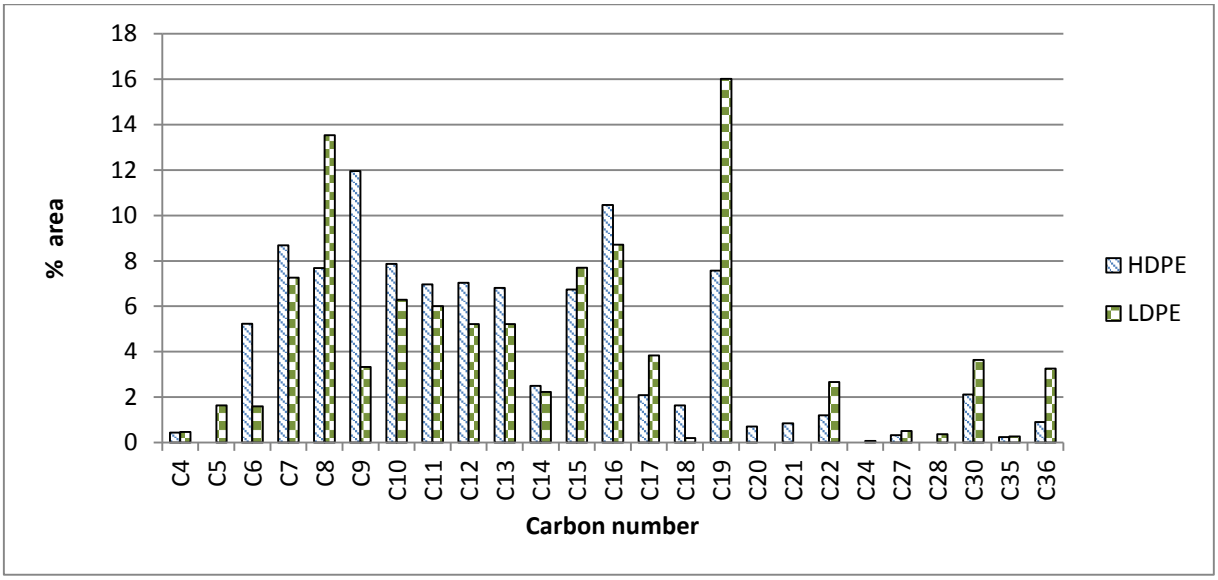

Figure 2: Carbon number distribution

The results of ATR the FT-IR spectra recorded for the obtained oils are presented in Figure 3.

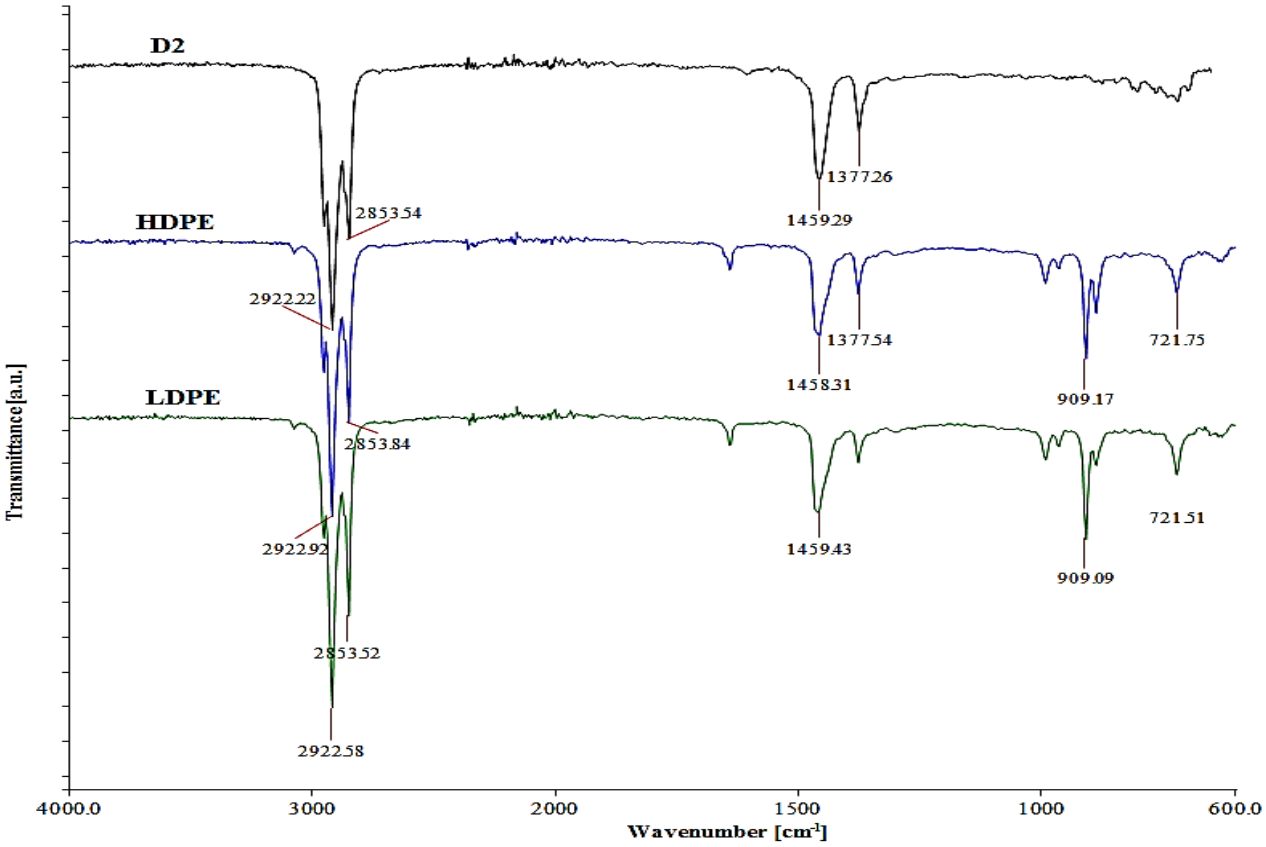

164

165 **Figure 3: ATR FT-IR spectra of conventional diesel fuel (D2) and the pyrolysis oils of HDPE and LDPE**

166 The ATR FTIR spectra of conventional diesel fuel (D2) and pyrolysis oils from HDPE and LDPE showed
167 the typical signals of aliphatic hydrocarbons in the range from 2960 cm^{-1} to 2850 cm^{-1}, at 1460 cm^{-1}
168 and at 1375 cm^{-1}, respectively, which are due to the presence of $-CH_3$ and $-CH_2$ groups. In addition to
169 the above signals, the typical signals for olefins were detected in the spectra of the pyrolysis oils of
170 HDPE and LDPE, at 3079 cm^{-1}, 1643 cm^{-1}, 991 cm^{-1} and 909 cm^{-1}. The mentioned signals were less
171 intense.

172 Fuels` properties for simulations

173 The properties of the fuel mixtures where calculated from the obtained properties of the HDPE and
174 LDPE pyrolytic oils presented in Table 1: Fuel properties [8]. Table 2 presents the properties of the
175 fuels that were used in the numerical simulations. According to [25] [26], a sharp drop of pressure at
176 the nozzle hole entry is so rapid that the absolute value of the fuel saturation pressure is of minor

influence on cavitation occurrence. Due to this finding, the saturation pressure for all fuels was the same.

Table 2: Fuel properties used in the simulations

	D2	HDPE	LDPE	HDPE_50	LDPE_50	HDPE_25	LDPE_25	HDPE_10	LDPE_10
Density at 15°C [kg/m^3]	830	770.40	775.40	800.20	802.70	815.10	816.35	824.04	824.54
Surface tension [mN/m]	26.8	23.20	23.00	25.00	24.90	25.90	25.85	26.44	26.42
Kin. Viscosity [mm2/s]	2.14	1.32	1.53	1.73	1.83	1.94	1.99	2.06	2.08

Experimental set-up

Injection system

A Denso diesel injector, model 7H150 with solenoid valve and seven injection holes, was used in the presented work. All injection holes had the same length of 0.76 mm and diameter of 0.15 mm. A detailed description of the experimental set-up was presented in [19].

Engine

The injector was taken from 4-cylinder Nissan YD22 enigine. The main properties of engine are presented in

Table 3: Properties of test engine

Properties	Value
Engine dssplacement [l]	2.184

Max. power [kW]	82 (@4000 min^{-1})
Max. torque [Nm]	248 (@2000 min^{-1})
Compression ratio	16.7/1
Bore [mm]	86.5
Stroke [mm]	94

Operating regime

The operating regimes were obtained during the experimental measurements. The selected engine operating regime for this work was 1700 rpm, 110 NM of torque, BMEP 6.33 bar, 845 bar of injection pressure and 60 bar of in-cylinder back pressure. The total injection time was 1.26 ms. [19,29,30]

Numerical model

Model

The numerical model was made for one injection hole (one seventh of the whole injector). Additional volume (marked with VOL on Figure 4) was placed at the outlet of the injection nozzle. The volume is used for boundary condition definition, and allows us to avoid defining the boundary condition at the nozzle hole exit. According to the program provider we get more realistic physical initialization and results at the nozzle outlet when using this method for outlet boundary condition definition.

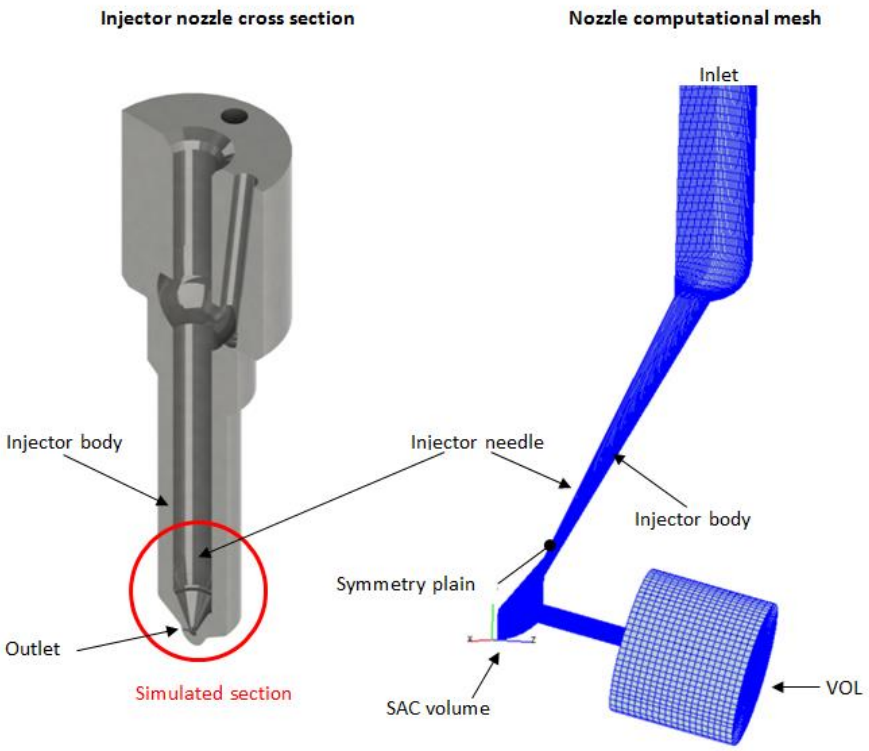

205

206 **Figure 4: Injector nozzle model cross-section and computational mesh**

207

208 Mesh independence study

209 The mesh independence study was carried out in order to estimate the numerical error. The
210 Richardson extrapolation method was used to determine the grid convergence index (GCI), which
211 provides a uniform measure of convergence for the grid refinement studies, and presents an
212 estimate of the discretization error. [31,32] The average fuel velocity and turbulent kinetic energy
213 (TKE) at the outlet were monitored on three different meshes with different numbers of elements.
214 The study was done with the injection needle half open. The results of the mesh independence study
215 are presented in Table 3.

216 **Table 4: Mesh independence study**

Mesh	Number of	Average velocity at the	Average turbulence kinetic energy at

	elements	outlet [m/s]	the outlet [J/kg]
Coarse (1)	138175	282.87	518.27
Medium (2)	358996	287.38	801.83
Fine (3)	1582816	257.46	856.25
GCI_{fine} [%]	-	4.26	0.541
GCI_{medium} [%]	-	1.23	9.06

217

218 Following the results of the mesh independence study, the medium mesh with 358,996 elements was
219 used for further work. The additional refinement of the mesh provides slightly better results, but
220 increases the calculation time significantly.

221 Simulation set-up

222 The time (physical) of simulation was equal to the total injection time obtained during the
223 experimental work. The time was 1.26 ms, and was the same for all the simulation. The timesteps in
224 the simulation where smaller at the start of simulation ($2.5x10^{-8}$ s) and larger ($5.0x10^{-8}$ s) at the end
225 of simulation. This configuration provided good convergence during the whole simulation. The
226 injection pressure of 845 bar was defined at the inlet. The in-cylinder back pressure of 60 bar was
227 defined in the volume (VOL) added to the numerical model of the injector. the symmetry boundary
228 condition was used on the sides of the injector body. The properties of the tested fuels are presented
229 in Table 1, and were implemented in the computational program.

The transient needle movement was defined during the simulation. The needle lift during the injection was the same for all fuels, and was defined in [19]. The needle lift process is split into three phases, and is presented in Figure 5. The first is the needle opening phase, which begins with the start of needle lift and ends at 0.6 ms when the needle is more than 95 % open. It is followed by the open phase, when needle is fully open (more than 95% of full needle lift). At 0.74 ms the closing phase of the needle lift starts, and ends with the needle being fully closed at 1.26 ms.

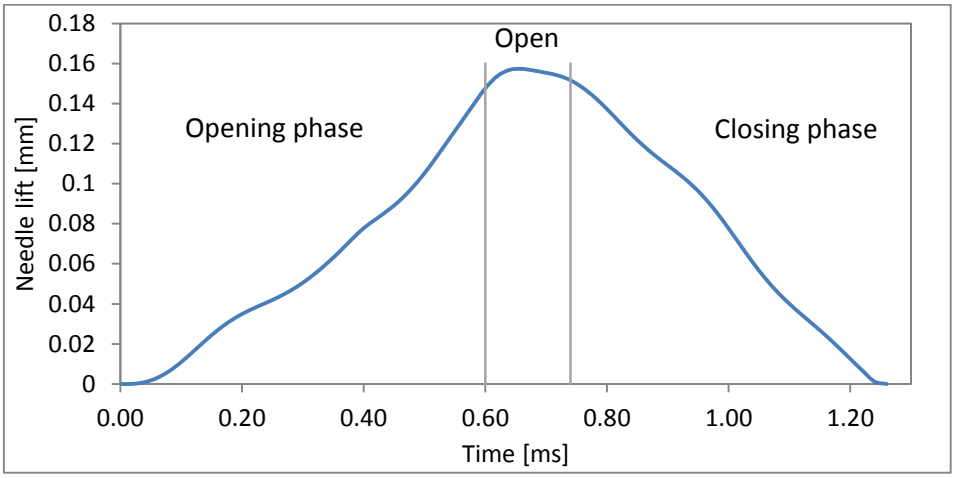

Figure 5: Needle lift

At the start of the simulation, the needle in the numerical model was not fully closed. This allowed avoiding the zero thickness cells, and enabled us to determine the computational mesh in the whole model. The minimal distance between the injector body and the needle was 1 µm.

Mathematical models

The simulations of unsteady, multi-phase flow inside the injector were performed using the Eulerian-Eulerian approach. The two-fluid model approach was used, which calculates all the conservation equations for each phase and is integrated in the AVL FIRE computational program. Mass (eq. (1)), momentum (eq. (2)) and energy (eq. (3)) conservation equations where considered during the calculation. Additional to the conservation equations, a Linear cavitation model was used to calculate the mass and momentum exchange on the phases` interface. The changes of fuel density with

248 pressure were calculated using the Tait equation (4), while turbulence modeling was done using a
249 standard k-ε turbulent model with hybrid wall treatment, which is suitable for all y+ values. [33] The
250 equations are presented in Table 4.

251 **Table 5: Used mathematical models** [33]

$\frac{\partial \alpha_k \rho_k}{\partial t} + \nabla \cdot \alpha_k \rho_k v_k = \sum_{l=1.l\neq k}^{2} \Gamma_{kl}$	Mass eq. (1)
$\frac{\partial \alpha_k \rho_k v_k}{\partial t} + \nabla \cdot \alpha_k \rho_k v_k v_k = -\alpha_k \nabla p + \nabla \cdot \alpha_k (\tau_k + \tau_k^t) + \alpha_k \rho_k g + v_k \sum_{l=1.l\neq k}^{2} \Gamma_{kl} + \sum_{l=1.l\neq k}^{2} \mathrm{M}_{kl}$	Momentum eq. (2)
$\frac{\partial \alpha_k \rho_k h_k}{\partial t} + \nabla \cdot \alpha_k \rho_k v_k h_k = \nabla \cdot \alpha_k (q_k + q_k^t) + \alpha_k \rho_k q_k''' + \alpha_k \rho_k f \cdot v_k + \nabla \cdot \alpha_k (\tau_k + \tau_k^t) \cdot v_k + \alpha_k \frac{\vartheta p}{\vartheta t} + \sum_{l=1.l\neq k}^{2} \mathrm{H}_{kl} + \sum_{l=1.l\neq k}^{2} \mathrm{h}_{ki} \Gamma_{kl}$	Energy eq. (3)
$\rho_l = \rho_{ref} \sqrt[\mathrm{n}]{\frac{p + \mathrm{B}}{p_{ref} + \mathrm{B}}}$	Tait eq. (4)

$\Gamma_{12} = \rho_d N''' 4\pi R^2 \dot{R} = \Gamma_{21}$	Interfacial mass exchange eq. (5)

252

253 **Results**

254 The following Section presents the results of fuel properties` influence on the injection properties
255 and in nozzle flow conditions in the used common rail diesel injector.

256 Figure 6 present the results of the total injected fuel mass for all tested fuels and for the
257 experimentally obtained results. Numerical (simulated) obtained results are marked with
258 abbreviation NS while experimental results are marked with abbreviation EXP.

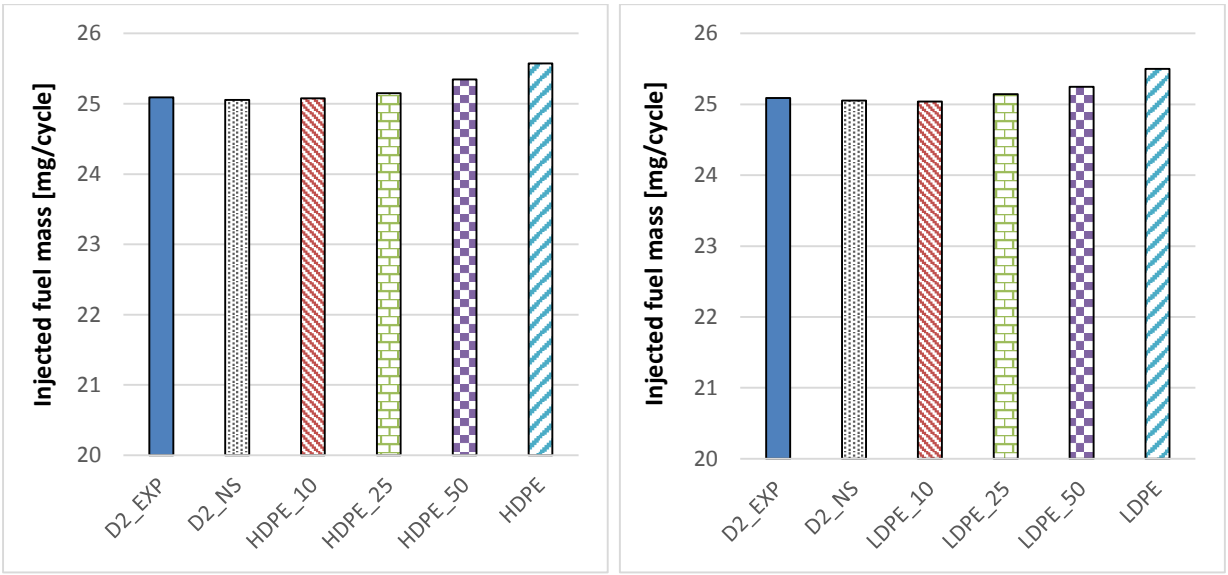

259 **Figure 6: Comparison of injected fuel mass**

260 From the results presented in Figure 6 we can see that the numerical simulation predicts the total
261 injected fuel mass in one injection cycle precisely. The difference between the numerical and
262 experimentally obtained results of total injected fuel mass for diesel fuel is less than 1 %. The

263 presented results also indicate that adding plastic derived fuel to diesel fuel has an influence on the
264 increased total injected fuel mass.

265 In-Nozzle Flow and Cavitation Inception

266 In the following chapter only the most relevant numerical results are presented at different times
267 during the injection process.

268 When fuel flows through the injection nozzle it undergoes significant changes which influence local
269 flow velocity and pressure. There are two distinctive areas where cavitation is usually formed. The
270 first is under the injection needle, where the cavitation is formed during an early stage of needle
271 opening and at the last steps of needle closing, due to the very narrow gap between the injector
272 needle and the needle seat. This gap increases fuel flow velocity and decreases its pressure, which
273 induces the formation of cavitation. The second area is at the injection hole entry, where the fuel
274 undergoes significant changes in flow direction: This from an area, usually in the upper part of the
275 injection nozzle hole, where the pressure drop is very high (almost to the value of 0 Pa of absolute
276 pressure [34]), and induces cavitation formation. In the presented study, we have focused only on
277 studying the cavitation formation in the injector`s injection hole.

278 Figure 7 present the time when cavitation structures are present in the computation domain of the
279 injector`s nozzle hole during the injection process.

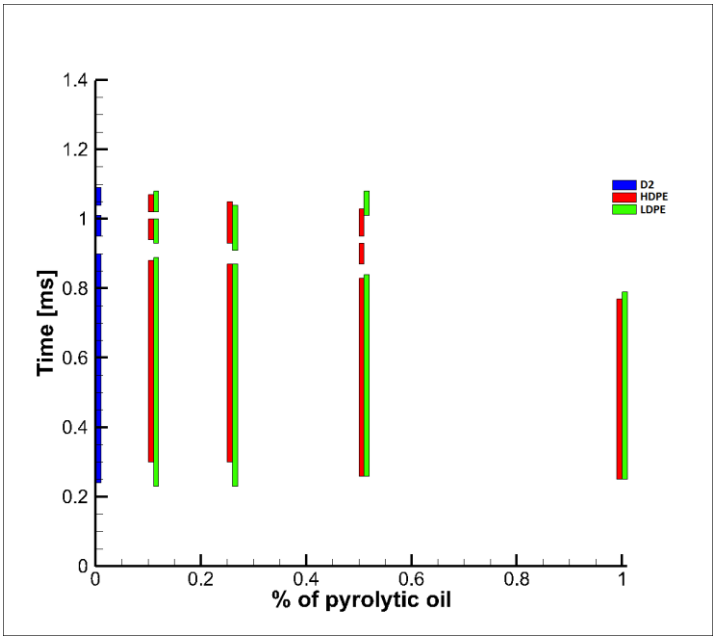

Figure 7: Appearance of cavitation in the injection hole

As can be seen from Figure 7, cavitation in the injection hole starts to form between 0.25 and 0.30 ms after the injection starts. Then it starts do dissipate (collapse) around 0.77 ms after the start of injection, and depending on the used fluid, reappears again after around 1 ms of the injection process. From the presented results we can see clearly that the cavitation inside the injection nozzle fluctuates during the closing phase of the injection process.

Needle opening phase

From the results presented in Figure 7 we can see that cavitation starts to form in the needle opening phase, and is present constantly for all fuels up to the needle closing phase.

Figure 8 and Figure 9 present the results of cavitation development on a plane positioned in the middle of the injection hole for the needle opening phase. The presentation plane is presented schematically in the upper right corner of all Figures presenting cavitation development on the middle plane of the nozzle injection hole. The results are presented for time intervals from 0.3 ms up to 0.64 ms of the needle opening phase, with time increments of 0.02 ms. Before 0.3 ms there was hardly any difference in the contours of the cavitation, so the results are not included. Only the

contours of cavitation structures are shown, for better presentation. This presentation gives us an insight into cavitation formation and spread through the injection hole during the needle opening phase.

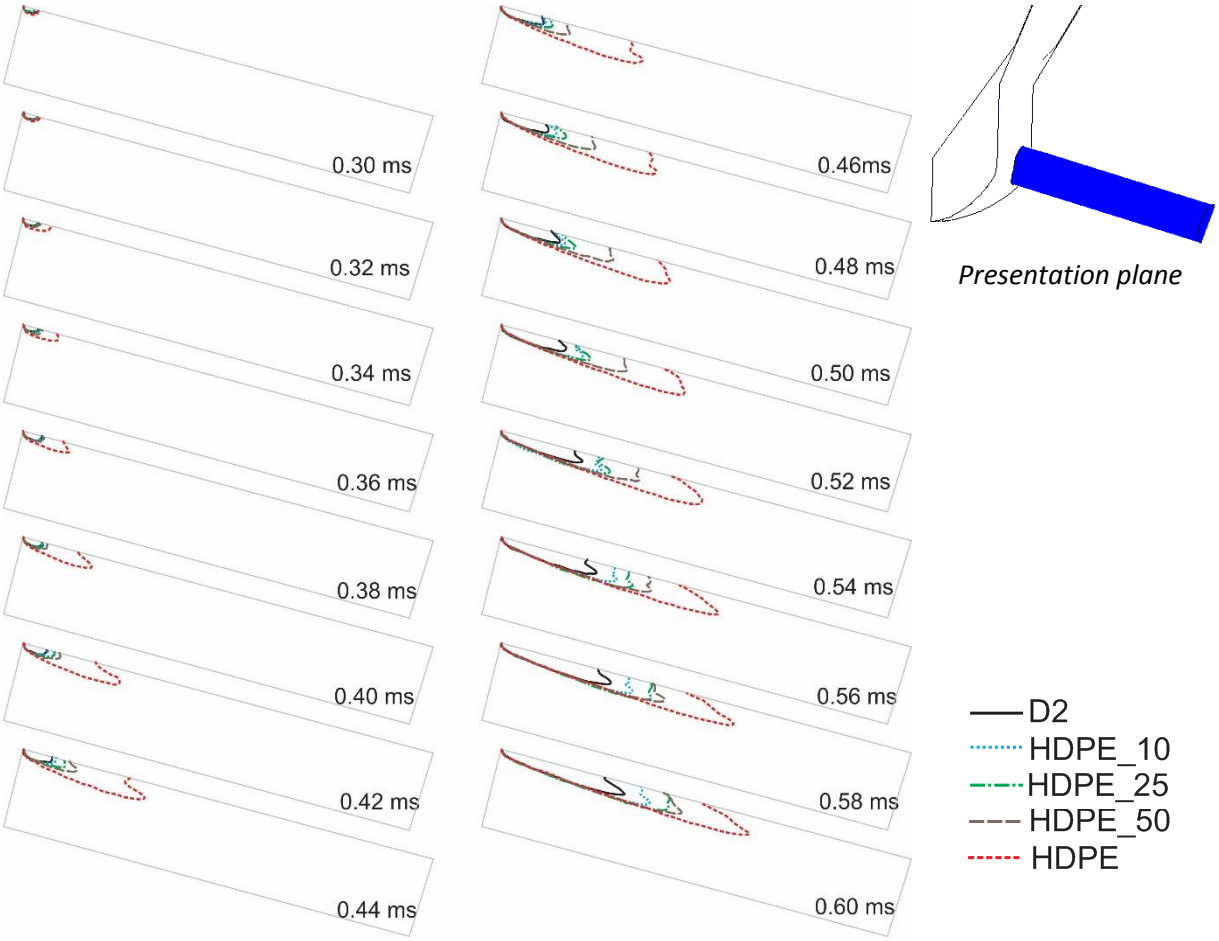

Figure 8: Contours of cavitation development for diesel fuel, HDPE fuel and their mixtures during the needle opening phase

The transition from non-cavitation to cavitating flow in the needle opening phase for diesel fuel, HDPE pyrolytic oil and their mixtures are presented in Figure 8. At 0.30 and 0.32 ms the contours for all fuels have the same shape and length. At 0.34 ms of injection time we obtained rapid formation and spread of cavitation contours for the HDPE oil, followed by significantly slower growth of

HDPE_50, HDPE_ 25, HDPE_10 and diesel fuel cavitation structures. The ratios between the tested fuels stayed more or less the same till the end of the needle opening phase. Since the boundary conditions in all simulations were the same, the difference in cavitation development was influenced by the differences in fuel properties. Pyrolytic oil and their mixtures have lower viscosity compared to diesel fuel, which can influence higher fuel velocity due to lower friction [23], while higher viscosity of diesel fuel also influences slower formation of cavitation structures in the needle opening phase. This influences faster formation and spread of plastic derived fuels` cavitation structures through the injection hole.

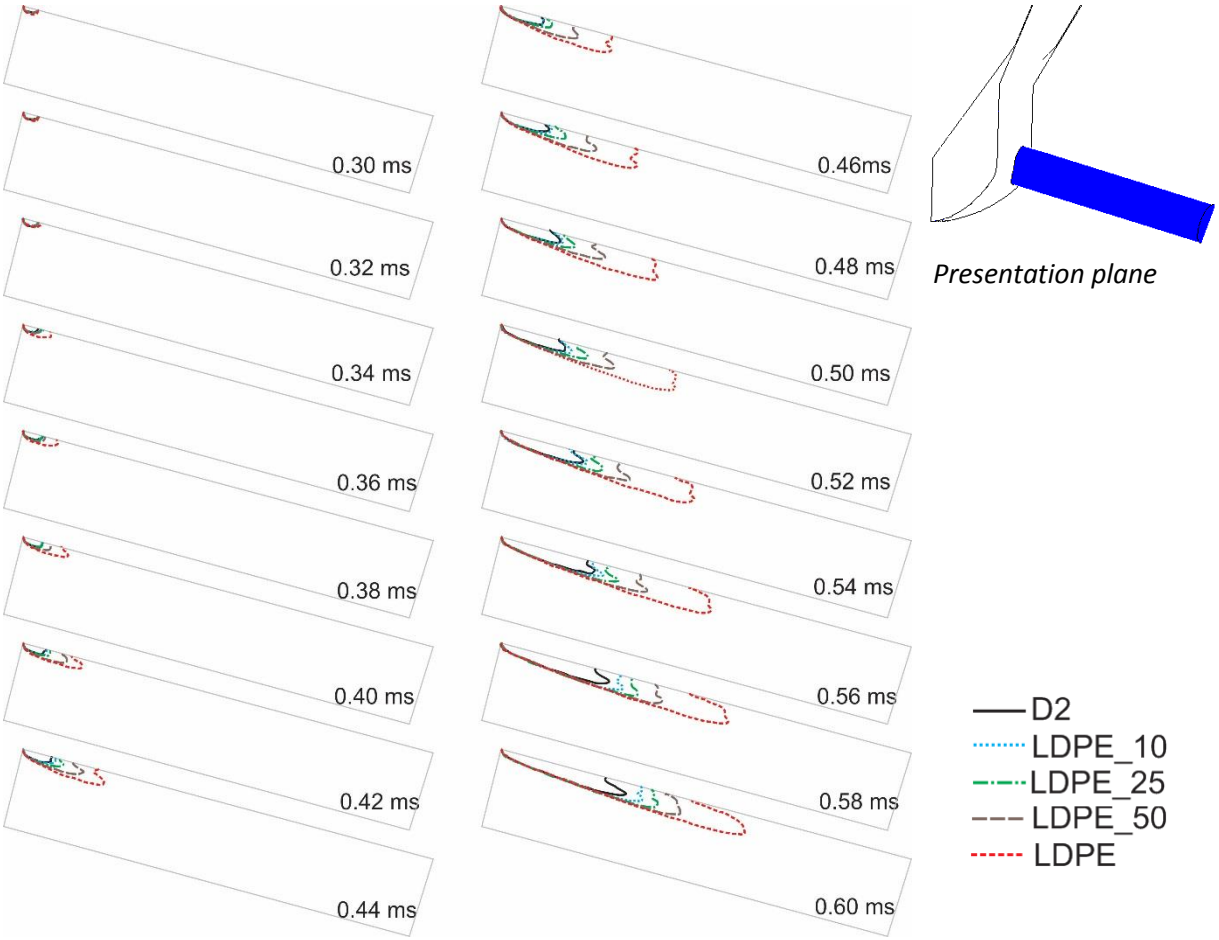

Figure 9: Contours of cavitation development for diesel fuel, LDPE fuel and their mixtures during the needle opening phase

The results for the cavitation development of LDPE pyrolytic oil and their mixture with diesel fuel, presented in Figure 9, show similar trends as the results for HDPE oil. The difference between the

cavitation structures` formation and spread through the injection hole started to occur at 0.36 ms of injection. The lower density and viscosity of LDPE pyrolytic oil influenced the faster formation and faster spread of cavitation structures through the injection hole. The longer cavitation structures of PO and its mixtures stayed present till the end of the needle opening phase.

Comparing the differences between pure pyrolytic oils, we can notice that the lower density and viscosity of HDPE pyrolytic oil influence the faster formation and spread of cavitation structures in the early stage of needle opening, up to 0.50 ms. From 0.52 ms on there was no visible difference in the length of the cavitation structures` contours for pure HDPE and LDPE pyrolytic oils.

Phase of open needle

The phase of open needle presents the time during the injection process when the needle is fully open (more than 95% of maximal needle lift). Figure 10 presents the contours of the cavitation structures in the nozzle hole for the HDPE and LDPE pyrolytic oils and their mixtures during the needle open phase.

a

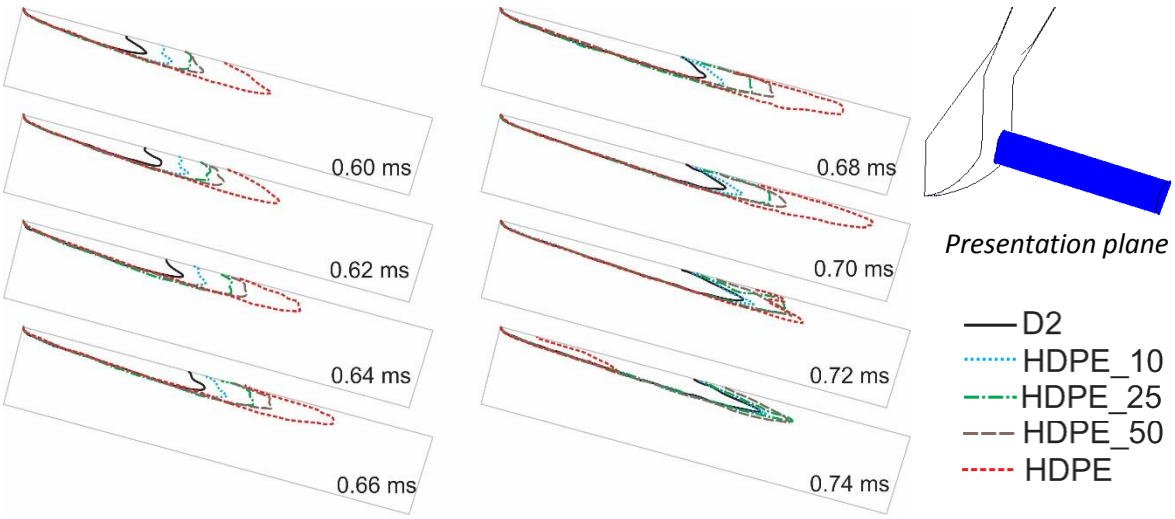

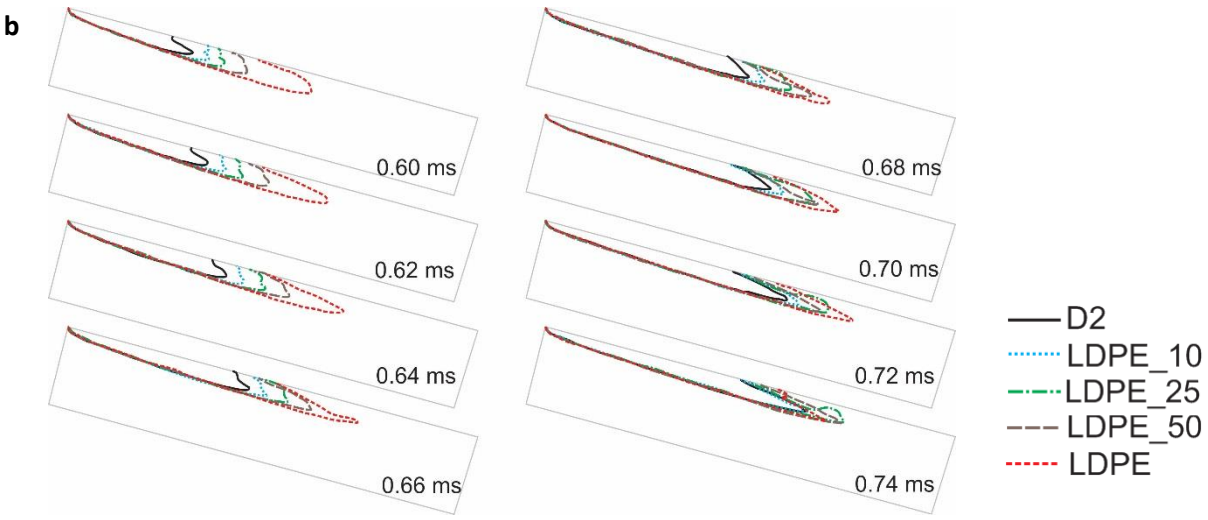

333 **Figure 10: Contours of cavitation development for diesel fuel, HDPE fuel (a), LDPE fuel (b) and their mixtures during the**
334 **phase of open needle**

335 The results presented in Figure 10 indicate that cavitation structures continue to form and spread
336 through the injection hole in the phase of open needle. This phenomenon is more rapid for fuels with
337 lower density and viscosity, which influence the time when each fuel obtains the maximal length of
338 cavitation structure. In Figure 10 a we can see that, for pure HDPE oil, this occurred at 0.70 ms after
339 the injection start, and for pure LDPE oil at 0.74 ms, Figure 10 b. The cavitation structures for all
340 other fuel mixtures and for pure D2 continued to grow and spread at the end of the needle open
341 phase.

342 ***Needle closing phase***

343 The last part of the injection process is the needle closing phase. The results of cavitation structures`
344 contours in this phase are presented in Figure 11 and Figure 12. Only results up to 1.08 ms are
345 presented, since there is no visible cavitation after that. After that there is no visible cavitation on the
346 presentation plane.

347

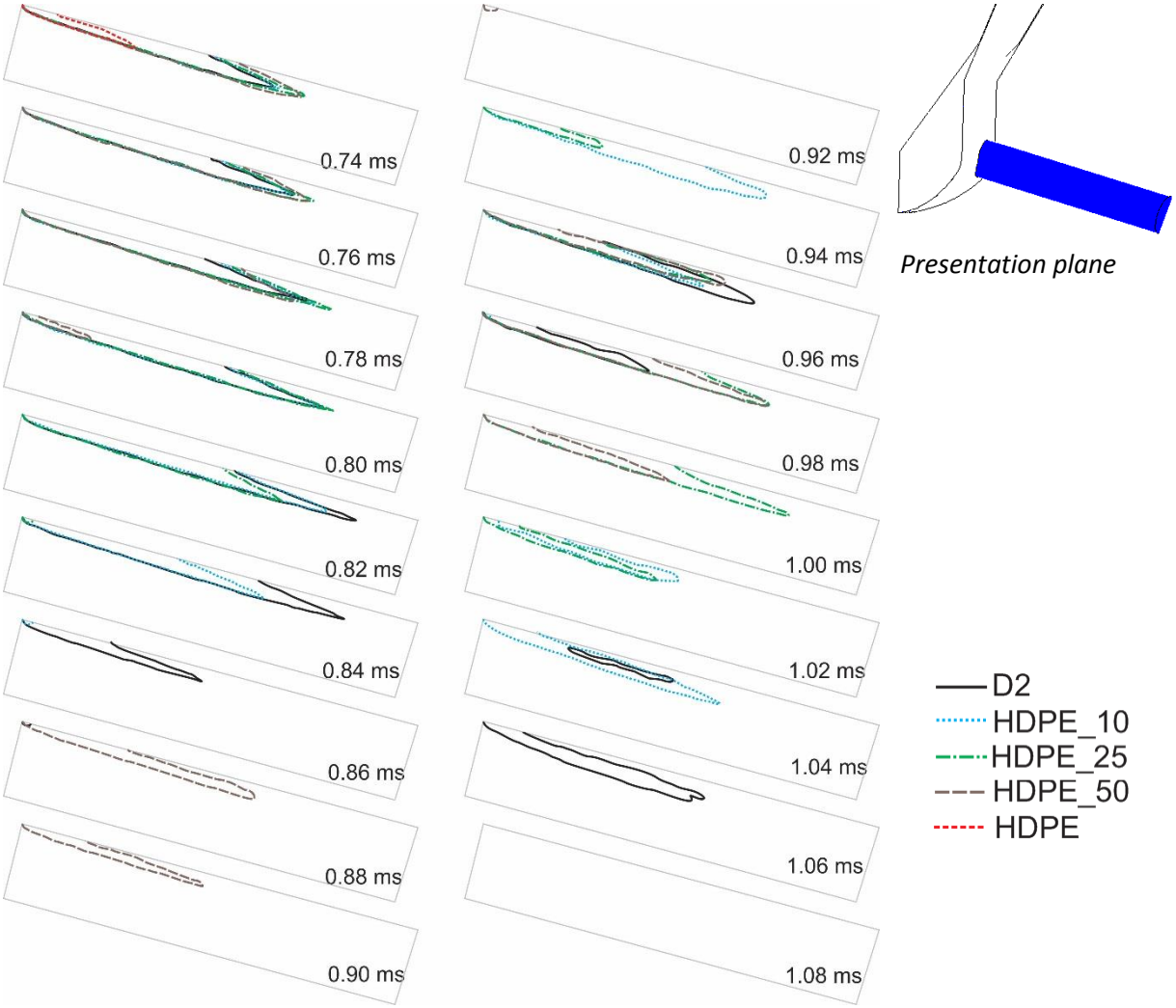

348 **Figure 11: Contours of cavitation development for diesel fuel, HDPE fuel and their mixtures during the needle closing**
349 **phase**

350 During the needle closing phase the cavitation structures for diesel fuel and for fuel mixtures
351 continued to form, and spread through the injection hole till they reached maximal length. For the
352 HDPE_50 mixture this occurred at 0.76 ms, for the HDPE_25 mixture at 0.78 ms, at 0.80 ms for the
353 HDPE_10 mixture, and at 0.82 ms for the pure diesel fuel. The growth and formation of cavitation
354 structures is again associated with the differences in fuels properties, and is more rapid for fuel
355 mixtures which have lower density and viscosity compared to pure diesel fuel, which is in line with
356 the results presented in [35]. The maximal length of cavitation structures is also influenced by fuel
357 properties. The presented results indicate that higher fuel density and viscosity increase cavitation
358 structure length, which was the longest for pure diesel fuel. Figure 11.

Once cavitation structures reach their maximal lengths they start to dissipate rapidly and dissipate completely in about 0.04 ms after they achieve maximal values. For pure diesel fuel, cavitation structure collapse occurs in 0.06 ms after maximal length. At 0.88 ms after the injection start the fluctuations of cavitation structures are visible in the injection hole at different times of the injection process for all fuel mixtures and for pure diesel fuel, but not for pure HDPE pyrolytic oil. Figure 11.

The same trends were also obtained for LDPE pyrolytic oil and its mixtures with diesel fuel. Figure 12. The cavitation structures for the pure LDPE_50 fuel mixture reached it maximal length at 0.76 ms, at 0.78 ms for LDPE_25, and at 0.82 ms for both LDPE_10 and pure diesel fuel. The longest cavitation structures where obtained for pure diesel fuel and its 10 % mixture with LDPE (LDPE_10), which again indicated that higher fuel density and viscosity increase the maximal length of the cavitation structures. The dissipation of cavitation structures again occurred in 0.04 ms after its maximal length was achieved for pure LDPE pyrolytic oil, and in 0.06 ms for pure diesel fuel and its mixtures with LDPE oil.

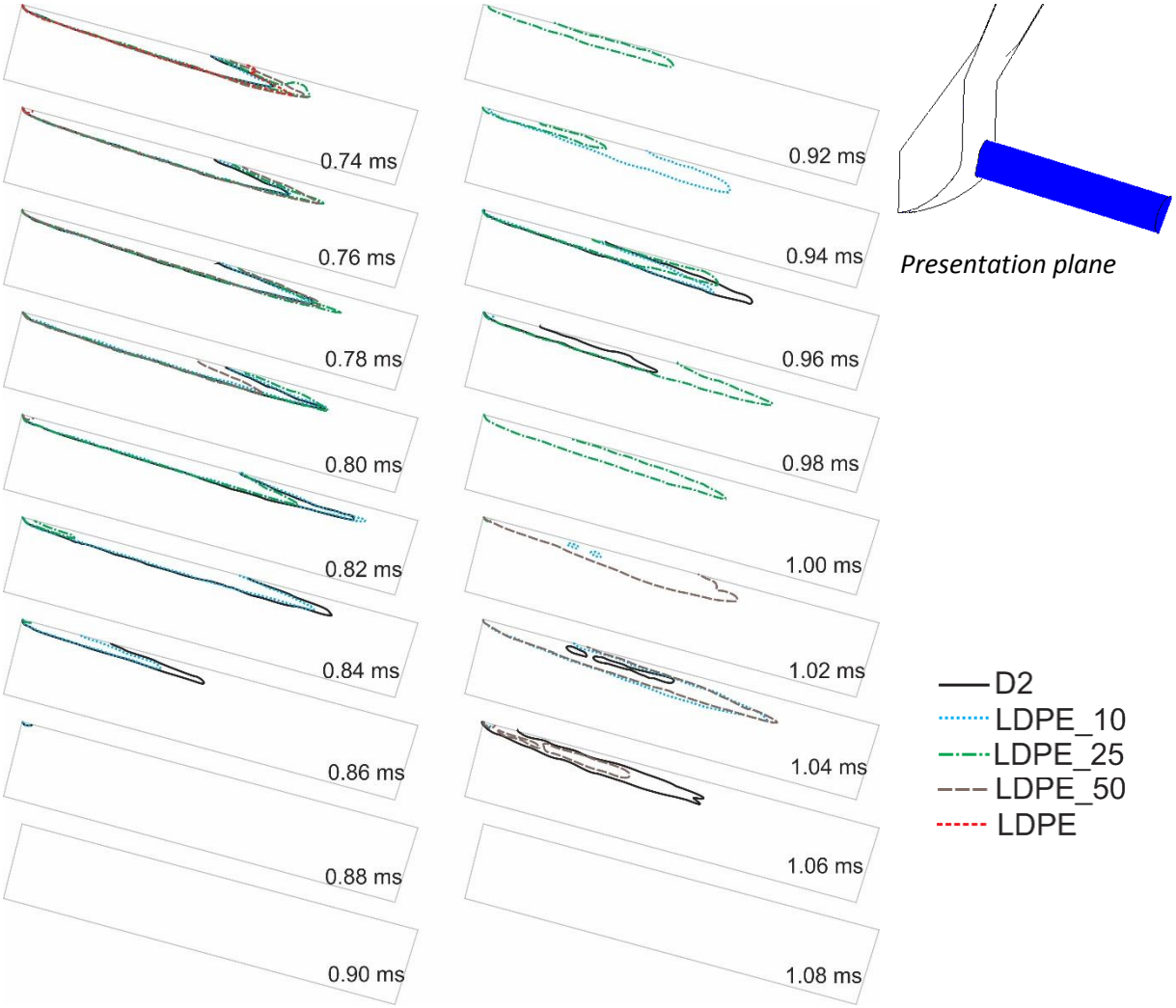

372 **Figure 12: Contours of cavitation development for diesel fuel, LDPE fuel and their mixtures during the needle closing**
373 **phase**

374 At 0.92 ms the fluctuation of the cavitation structures were again visible in the injection hole at
375 different times of the injection process for all fuel mixtures and for pure diesel fuel, but not for pure
376 LDPE pyrolytic oil. Figure 12. The differences in flow conditions in the injection hole during the needle
377 closing phase for different fuel were also observed in [25]. The authors of this study concluded that
378 fuel with lower density and lower viscosity responds faster to needle motion (closing) and behaves
379 less inertly compared to fuel with higher density and higher viscosity. They associated this
380 phenomenon to less resistance of fuel to disturbance if its viscosity is lower. Since the HDPE and
381 LDPE pyrolytic oils have significantly lower fuel viscosity compared to diesel fuel, they are less

382 resistant to disturbances in fuel flow caused by needle closing, which we believe results in no
383 cavitation fluctuation in the final stage of the needle closing phase.

384 Since the cavitation structures are present longer into the needle closing phase when fuel density
385 and viscosity are higher due to their later appearance, the choked flow, caused by the cavitation
386 cloud, is still present in the injection hole when the fuel flow starts do decline due to needle closing.
387 The choked flow can cause a local increase in fuel flow velocity, which can further influence the
388 pressure field inside the nozzle hole. So, the combined effects of fuel density influence on resistance
389 to disturbance to needle closing and later appearance of cavitation structures in the needle closing
390 phase, can influence rebound cavitation. This can be seen as fluctuation of the cavitation structures
391 close to the injection hole walls. This phenomenon is commonly seen in bubble collapse near the
392 wall. [36]

393 Nozzle hole exit

394 The conditions at the nozzle hole exit are very important, since they have a high influence on fuel
395 spray development and break-up. The disturbances of fuel flow at the nozzle hole exit are the results
396 of fuel flow upstream conditions and cavitation inception.

397 Figure 13 and Figure 14 resent the integral values of the fuel mass flow rate, the average value of
398 turbulent kinetic energy (AVR TKE), the maximal values of vapor volume fraction - cavitation phase
399 (MAX VVF), and the average values of normal velocity for one injection hole exit.

a b

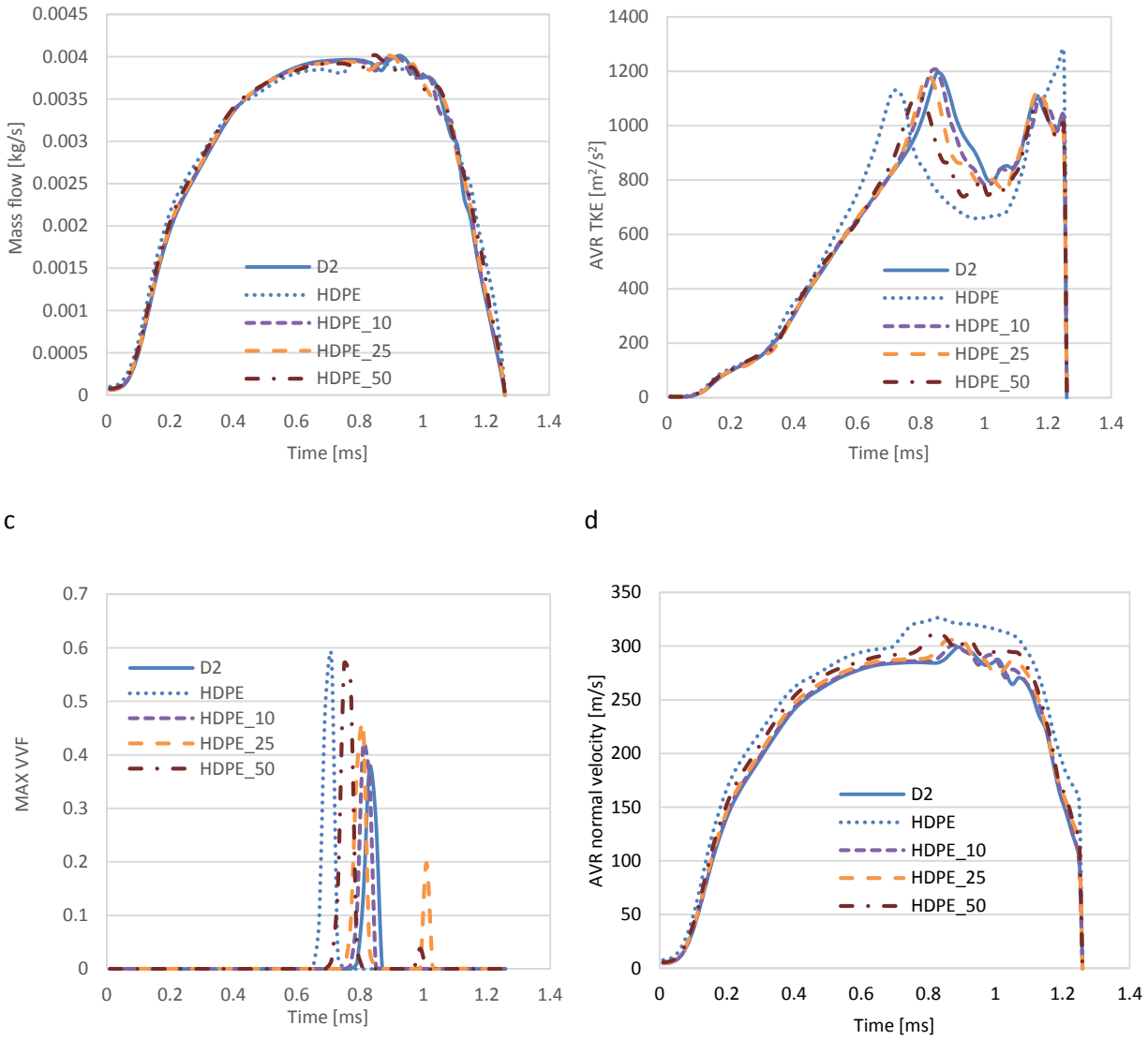

Figure 13: Outlet integral quantities for one injection hole (a) Mass flow rate; (b) Average value of fuel turbulent kinetic energy; (c) Maximal value of Vapor Volume Fraction; (d) Average normal velocity for HDPE fuel and their mixtures

The results for the fuel mass flow of pure HDPE oil and their mixtures with diesel fuel are presented in Figure 13. As we can see from the results, there is no significant difference for the mass flows of pure diesel, pure HDPE oil and their mixtures. In the needle opening phase, the mass flow for all fuels is increasing without fluctuations, in addition to which, mass flows for all fuels are steady without fluctuations, except for pure HDPE, where fluctuations in the mass flow rate started to occur at the end of the needle open phase. In the needle closing phase, the mass flow rate for all fuels started to decrease due to needle closing. There are visible fluctuations in all fuels` mass flows. The amplitudes

410 of fluctuations are the highest for pure diesel fuel, followed by fuel mixtures and pure HDPE oil. The
411 timing of mass flow fluctuations coincides with the occurrence of cavitation structures at the nozzle
412 hole exit (Figure 13 c). Since the maximal values of VVF for pure diesel fuel and fuel mixture are
413 smaller compared to pure HDPE fuel (Figure 13 c), the authors assume that the amplitudes of
414 fluctuations also depend on the fuel properties.

415 The cavitation phase occurs at the needle hole exit at different times, depending on the fuel. It first
416 appeared for pure HDPE oil, followed by HDPE_50, HDPE 25, HDPE_10 fuel mixtures, and, at the end,
417 by pure diesel fuel. The results coincide with the results of cavitation formation inside the injection
418 hole, where the cavitation started to form first for fuel with lower density and viscosity.

419 The results also show that the average values of fuels TKE increases with the increase of fuels` mass
420 flow rates, and that the peaks of the average TKE at the nozzle hole exit coincides with the time of
421 cavitation structures` occurrence at the nozzle hole exit. This indicates that the formation and spread
422 of cavitation structures influence the increased fuel TKE at the nozzle hole exit. The same trend is
423 evident for the fuel normal velocity at the nozzle hole exit. When cavitation structures occur at the
424 nozzle exit, high fluctuation are obtained in the fuels` normal velocity. The results also show that the
425 velocities for pure HDPE oil and their mixtures are higher than for pure diesel fuel. This is because of
426 the low viscosity of pyrolytic oil and its mixtures, which decreasethe friction of the fuel flow. This
427 phenomenon also explains why there are no significant difference in the fuels` mass flow rates.

a b

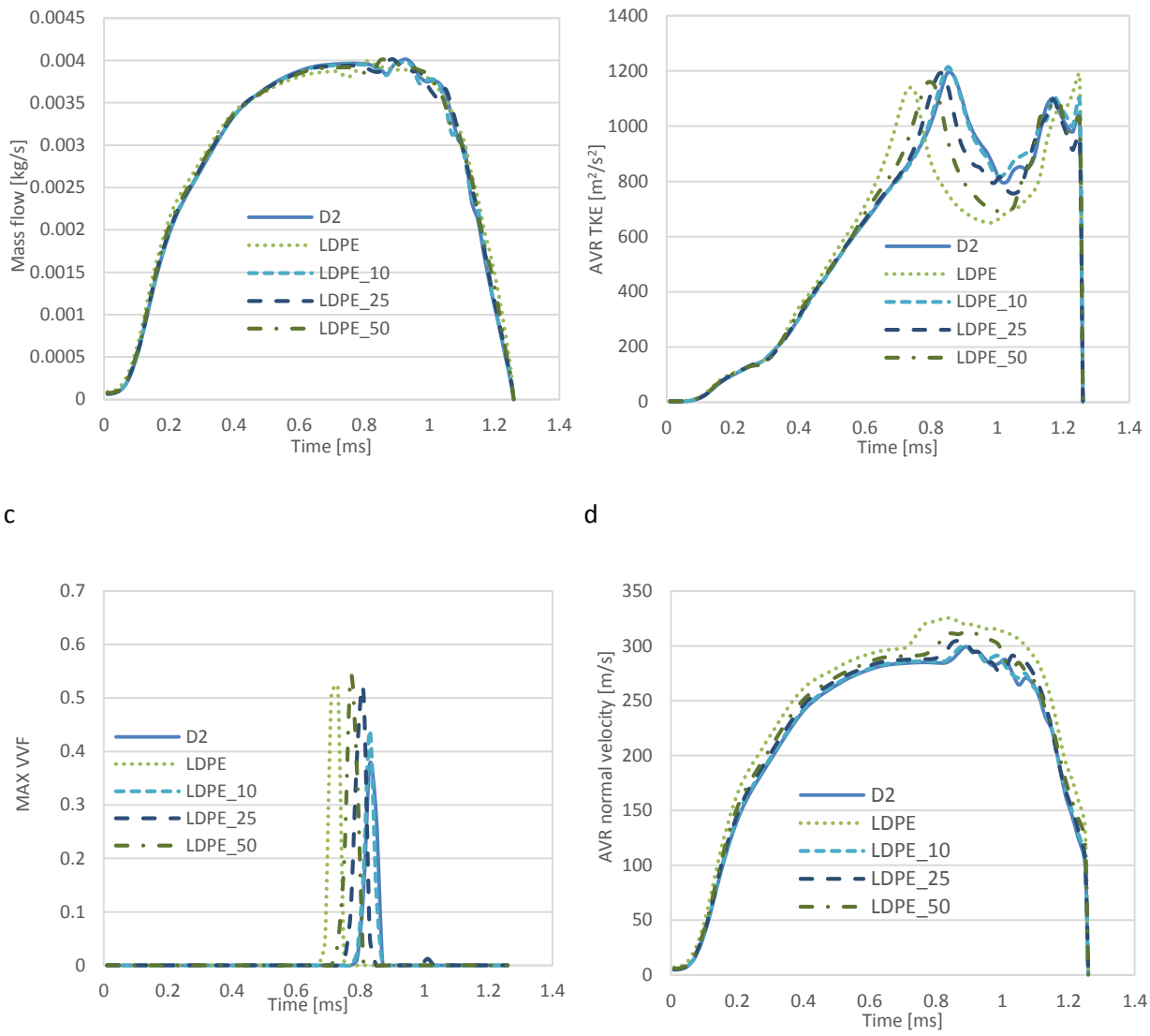

Figure 14: Outlet integral quantities for one injection hole (a) Mass flow rate; (b) Average value of fuel turbulent kinetic energy; (c) Maximal value of Vapor Volume Fraction; (d) Average normal velocity for LDPE fuel and their mixtures

The same trends are also seen for LDPE oil and their mixtures with diesel fuel Figure 14. During the needle opening phase the mass flow of fuels increases without any fluctuations in fuel flow. For pure LDPE pyrolytic oil the fluctuations in fuel mass flow occurred in the needle open phase, while, for other fuels, at the start of the needle closing phase. The values of fuels` average normal velocity and turbulent kinetic energy at the injection hole exit again increased with the increase in the fuels` mass flow rate. The peak values of average normal velocity and TKE at the hole exit again coincides with the time of the cavitation structures` occurrence. Figure 14 c indicates that cavitation influences conditions at the injection hole exit, and can influence fuel spray break-up further.

The timing of cavitation occurrence at the injection hole exit again depends on the fuel, and coincides with the results of cavitation formation inside the injection hole for each tested fuel. This indicates that lower fuel density and viscosity not only influence on cavitation formation inside the injection hole, but also influence cavitation occurrence at the nozzle hole exit.

The scond peak of TKE on Figure 13 b and Figure 14 b can be related to needle closing and late appearance of cavitation structures in needle closing phase. During the needle closing phase fluctuation in fuel flow can occur due to needle closing and can further results in second peak of TKE, which is the highes in time of needle being almost fully closed.

Conclusions

In the presented paper the influence of pyrolytic oils, produced from waste plastic, were tested numerically on fuel flow conditions inside the injection nozzle of a solenoid injector. First pyrolytic oils were produced from waste HDPE and LDPE plastic using a single batch pyrolytic reactor. Then, the properties of the obtained oils were determined using different test methods. The obtained oils` properties were used further to specify 10%, 25% and 50% fuels mixtures properties with conventional diesel fuel. All properties were further implemented in the AVL FIRE computational program and used in the numerical study. The main conclusions from the presented study are:

- Pyrolytic oils obtained from waste HDPE and LDPE plastic have similar properties to conventional diesel fuel.
- The lower viscosity of pyrolytic oils influences lower friction in the fuel nozzle flow, which influences higher fuel velocity and compensates the lower fuel density`s influence on the total injected fuel mass and mass flow rate.
- The lower density and viscosity of pyrolytic oils influence the more rapid formation and spread of cavitation structures.
- Fuels with lower viscosity and density increase the amount of cavitation (vapor volume fraction) at the injection hole exit and advance the time of its appearance.

- During the needle opening phase there is no significant difference at the nozzle hole outlet, regardless of the fuel properties.
- The lower fuel viscosity and density of pure pyrolytic oils influence the shorter presence of cavitation in the needle closing phase, lower resistance to disturbance and less choked flow in the needle closing phase, which resulst in flow without cavitation fluctuation.
- Higher fuel viscosity and density influence the rebound cavitation formation close to the injection hole walls.

From the presented study we can conclude that fuel properties have a significant influence on flow conditions and cavitation formation inside the nozzle injection hole and at its exit. This can further influence the spray break-up process, which is crucial for clean combustion optimal engine performance. Cavitation structures can appear at the nozzle hole exit early in the injection process, which can occur if pyrolytic oils are used. They can influence the faster decline of the spray axis, which can cause formation of an asymmetrical fuel spray and increase the possibility for spray collision with other spray or combustion chamber walls. The occurrence and fluctuation of cavitation in the injection nozzle also influences the erosion of the injection hole. The erosion potential of each fuel will be studied in further work.

Finally, the presented study indicates that plastic waste can be used for resource recovering, and can help to reduce the environmental impact of plastic usage. In the presented study, we have confirmed that high density and low density polyethylene can be converted into oils with similar properties to conventional fuels using the pyrolytic process. The obtained pyrolytic oils can be used as a substitute to conventional diesel fuel, but, due to their influence on the injection process, further studies are needed before implementation.

Acknowledgements

The authors wish to thank the Slovenian Research Agency (ARRS) for the financial support in the framework of the Research Programme P2-0196 in Power, Process and Environmental Engineering and P2-0118 Textile Chemistry. This work was supported by the Spanish Ministry of Science, Innovation, and Universities [RTI2018-095923-B-C21].

References

[1] Association of Plastic Manufacturers (Organization). Plastics – the Facts 2020. PlasticEurope 2020:16.

[2] Lee S, Yoshida K, Yoshikawa K. Application of Waste Plastic Pyrolysis Oil in a Direct Injection Diesel Engine: For a Small Scale Non-Grid Electrification. Energy Environ Res 2015;5:18–32. https://doi.org/10.5539/eer.v5n1p18.

[3] Bai B, Jin H, Fan C, Cao C, Wei W, Cao W. Experimental investigation on liquefaction of plastic waste to oil in supercritical water. Waste Manag 2019;89:247–53. https://doi.org/10.1016/j.wasman.2019.04.017.

[4] Plastics Europe GMR, Conversio Market & Strategy GmbH. Plastics - the Facts 2019 2019:14, 35.

[5] Khoo KS, Ho LY, Lim HR, Leong HY, Chew KW. Plastic waste associated with the COVID-19 pandemic: Crisis or opportunity? J Hazard Mater 2021;417:126108. https://doi.org/10.1016/j.jhazmat.2021.126108.

[6] Potrykus M, Redko V, Głowacka K, Piotrowicz-Cieślak A, Szarlej P, Janik H, et al. Polypropylene structure alterations after 5 years of natural degradation in a waste landfill. Sci Total Environ 2021;758. https://doi.org/10.1016/j.scitotenv.2020.143649.

[7] Zhang F, Zhao Y, Wang D, Yan M, Zhang J, Zhang P, et al. Current technologies for plastic waste treatment: A review. J Clean Prod 2021;282:124523. https://doi.org/10.1016/j.jclepro.2020.124523.

[8] Kassargy C, Awad S, Burnens G, Kahine K, Tazerout M. Gasoline and diesel-like fuel production by continuous catalytic pyrolysis of waste polyethylene and polypropylene mixtures over USY zeolite. Fuel 2018;224:764–73. https://doi.org/10.1016/j.fuel.2018.03.113.

[9] Kassargy C, Awad S, Burnens G, Kahine K, Tazerout M. Experimental study of catalytic pyrolysis of polyethylene and polypropylene over USY zeolite and separation to gasoline and diesel-like fuels. J Anal Appl Pyrolysis 2017;127:31–7. https://doi.org/10.1016/j.jaap.2017.09.005.

[10] Jeon W, Kim YD, Lee KH. A comparative study on pyrolysis of bundle and fluffy shapes of waste packaging plastics. Fuel 2021;283:119260. https://doi.org/10.1016/j.fuel.2020.119260.

[11] Anuar Sharuddin SD, Abnisa F, Wan Daud WMA, Aroua MK. A review on pyrolysis of plastic wastes. Energy Convers Manag 2016;115:308–26. https://doi.org/10.1016/j.enconman.2016.02.037.

[12] Mangesh VL, Padmanabhan S, Tamizhdurai P, Narayanan S, Ramesh A. Combustion and emission analysis of hydrogenated waste polypropylene pyrolysis oil blended with diesel. J Hazard Mater 2020;386:121453. https://doi.org/10.1016/j.jhazmat.2019.121453.

[13] Kizza R, Banadda N, Seay J. Qualitative and energy recovery potential analysis: plastic-derived fuel oil versus conventional diesel oil. Clean Technol Environ Policy 2021. https://doi.org/10.1007/s10098-021-02028-9.

[14] Tulashie SK, Boadu EK, Dapaah S. Plastic waste to fuel via pyrolysis: A key way to solving the severe plastic waste problem in Ghana. Therm Sci Eng Prog 2019;11:417–24. https://doi.org/10.1016/j.tsep.2019.05.002.

[15] Mangesh VL, Padmanabhan S, Tamizhdurai P, Ramesh A. Experimental investigation to identify the type of waste plastic pyrolysis oil suitable for conversion to diesel engine fuel. J Clean Prod 2020;246:119066. https://doi.org/10.1016/j.jclepro.2019.119066.

[16] Singh TS, Verma TN, Singh HN. A lab scale waste to energy conversion study for pyrolysis of plastic with and without catalyst: Engine emissions testing study. Fuel 2020;277:118176.

https://doi.org/10.1016/j.fuel.2020.118176.

[17] Das AK, Hansdah D, Mohapatra AK, Panda AK. Energy, exergy and emission analysis on a DI single cylinder diesel engine using pyrolytic waste plastic oil diesel blend. J Energy Inst 2020;93:1624–33. https://doi.org/10.1016/j.joei.2020.01.024.

[18] Singh RK, Ruj B, Sadhukhan AK, Gupta P, Tigga VP. Waste plastic to pyrolytic oil and its utilization in CI engine: Performance analysis and combustion characteristics. Fuel 2020;262:116539. https://doi.org/10.1016/j.fuel.2019.116539.

[19] Lešnik L, Kegl B, Torres-Jiménez E, Cruz-Peragón F, Mata C, Biluš I. Effect of the in-cylinder back pressure on the injection process and fuel flow characteristics in a common-rail diesel injector using gtl fuel. Energies 2021;14. https://doi.org/10.3390/en14020452.

[20] Lešnik L, Kegl B, Bombek G, Hočevar M, Biluš I. The influence of in-nozzle cavitation on flow characteristics and spray break-up. Fuel 2018;222. https://doi.org/10.1016/j.fuel.2018.02.144.

[21] Cristofaro M, Edelbauer W, Koukouvinis P, Gavaises M. A numerical study on the effect of cavitation erosion in a diesel injector. Appl Math Model 2020;78:200–16. https://doi.org/10.1016/j.apm.2019.09.002.

[22] Yu W, Yang W, Zhao F. Investigation of internal nozzle flow, spray and combustion characteristics fueled with diesel, gasoline and wide distillation fuel (WDF) based on a piezoelectric injector and a direct injection compression ignition engine. Appl Therm Eng 2017;114:905–20. https://doi.org/10.1016/j.applthermaleng.2016.12.034.

[23] Torelli R, Som S, Pei Y, Zhang Y, Traver M. Influence of fuel properties on internal nozzle flow development in a multi-hole diesel injector. Fuel 2017;204:171–84. https://doi.org/10.1016/j.fuel.2017.04.123.

[24] Jiang G, Zhang Y, Wen H, Xiao G. Study of the generated density of cavitation inside diesel nozzle using different fuels and nozzles. Energy Convers Manag 2015;103:208–17. https://doi.org/10.1016/j.enconman.2015.06.065.

[25] Schwarz P, Blume M, Weiß L, Wensing M, Skoda R. 3D simulation of a ballistic direct injection cycle for the assessment of fuel property effects on cavitating injector internal flow dynamics and primary breakup. Fuel 2022;308:121775. https://doi.org/10.1016/j.fuel.2021.121775.

[26] Battistoni M, Grimaldi CN. Numerical analysis of injector flow and spray characteristics from diesel injectors using fossil and biodiesel fuels. Appl Energy 2012;97:656–66. https://doi.org/10.1016/j.apenergy.2011.11.080.

[27] Boichenko S. Manual. 2018.

[28] Altin O, Eser S. Carbon deposition from thermal stressing of petroleum fuels. ACS Natl Meet B Abstr 2004;228.

[29] Soriano JA, Mata C, Armas O, Ávila C. A zero-dimensional model to simulate injection rate from first generation common rail diesel injectors under thermodynamic diagnosis. Energy 2018;158:845–58. https://doi.org/10.1016/j.energy.2018.06.054.

[30] Soriano JA, García-Contreras R, Leiva-Candia D, Soto F. Influence on Performance and Emissions of an Automotive Diesel Engine Fueled with Biodiesel and Paraffinic Fuels: GTL and Biojet Fuel Farnesane. Energy and Fuels 2018;32:5125–33. https://doi.org/10.1021/acs.energyfuels.7b03779.

[31] Celik IB, Ghia U, Roache PJ, Freitas CJ, Coleman H, Raad PE. Procedure for estimation and reporting of uncertainty due to discretization in CFD applications. J Fluids Eng Trans ASME 2008;130:0780011–4. https://doi.org/10.1115/1.2960953.

[32] Boache PJ. Perspective: A method for uniform reporting of grid refinement studies. J Fluids

584 Eng Trans ASME 1994;116:405–13. https://doi.org/10.1115/1.2910291.

585 [33] Multiphase E. Avl fire ® version 2014.1 2014.

586 [34] Battistoni M, Som S, Powell CF. Highly resolved Eulerian simulations of fuel spray transients in
587 single and multi-hole injectors: Nozzle flow and near-exit dynamics. Fuel 2019;251:709–29.
588 https://doi.org/10.1016/j.fuel.2019.04.076.

589 [35] Wei M, Gao Y, Yan F, Chen L, Feng L, Li G, et al. Experimental study of cavitation formation
590 and primary breakup for a biodiesel surrogate fuel (methyl butanoate) using transparent
591 nozzle. Fuel 2017;203:690–9. https://doi.org/10.1016/j.fuel.2017.05.022.

592 [36] Yin J, Zhang Y, Zhu J, Lv L, Tian L. An experimental and numerical study on the dynamical
593 behaviors of the rebound cavitation bubble near the solid wall. Int J Heat Mass Transf
594 2021;177. https://doi.org/10.1016/j.ijheatmasstransfer.2021.121525.

595